

Space and Time pattern of mid-velocity IMF emission in peripheral heavy-ion collisions at Fermi energies

S. Piantelli, L. Bidini, G. Poggi, M. Bini, G. Casini, P.R. Maurenzig, A. Olmi, G. Pasquali, A.A. Stefanini and N. Taccetti

Istituto Nazionale di Fisica Nucleare and Università di Firenze, I-50125 Florence, Italy

(October 25, 2018)

The emission pattern in the $V_{perp} - V_{par}$ plane of Intermediate Mass Fragments with $Z=3-7$ (IMF) has been studied in the collision $^{116}\text{Sn} + ^{93}\text{Nb}$ at 29.5 AMeV as a function of the Total Kinetic Energy Loss of the reaction. This pattern shows that for peripheral reactions most of IMF's are emitted at mid-velocity. Coulomb trajectory calculations demonstrate that these IMF's are produced in the early stages of the reaction and shed light on geometrical details of these emissions, suggesting that the IMF's originate both from the neck and the surface of the interacting nuclei.

25.70.Lm, 25.70.Pq

An intense emission of intermediate mass fragments (IMF) at mid-velocity has been put into evidence [1,2,3,4,5,6,7] in collisions of heavy ions in the *Fermi regime*, i.e. at bombarding energies from 30 to 50 AMeV. For non-central collisions, where the binary character of the reaction is preserved, the mid-velocity particles are easily identified in the $V_{perp} - V_{par}$ plots, the velocity components being usually defined with respect to the separation axis of the two heavy reaction partners. The velocity region between target and projectile presents an intensity of particles unexpected on the basis of the statistical emission from the hot, fully accelerated main fragments. The multiplicity of mid-velocity particles is usually obtained by subtracting from the total emission the contribution of particles statistically emitted by the projectile- and target-like fragments (PLF and TLF), see [6,7]. Presently, the isospin composition of the mid-velocity light charged particles ($Z \leq 2$, LCP) and IMF's is highly debated, as it can be related to the composition of the emitting source, the so-called *neck* (see, e.g., [8] and references therein). Equally debated is the issue of the mechanism responsible for these mid-velocity emissions, namely whether they are of dynamical origin or due to an exotic statistical process, induced by perturbations of the Coulomb field [9].

It was shown by the INDRA collaboration [7] that, for a given bombarding energy, the largest ratio (up to ≈ 3) of *mid-velocity* to *statistical* IMF's is found in non-central collisions. However, due the relatively high thresholds for TLF detection of the existing 4π detectors, up to now the very peripheral collisions could not be reliably selected and the mid-velocity emission of IMF's was never cleanly isolated from the accompanying statistical emission, thus

preventing a detailed study of its characteristics.

In this Letter we present experimental results which, thanks to an efficient selection of peripheral reactions, make it possible to clearly isolate the mid-velocity emitted IMF's from the statistical component. The obtained selection allows -for the first time- to identify reactions where almost all IMF's concentrate at mid-velocity and to carefully study their emission pattern. Preliminary results were presented in Ref. [8].

The experiment (*Florentine Initiative After Superconducting Cyclotron Opening*, FIASCO) was performed at the *Laboratori Nazionali del Sud* in Catania (Italy). Targets of ^{93}Nb ($\approx 200 \mu\text{g}/\text{cm}^2$ thick) were bombarded with a 29.5 AMeV pulsed beam of ^{116}Sn of ≤ 0.1 nA intensity and ≤ 1 ns time resolution. The setup basically consisted of 24 position-sensitive Parallel Plate Avalanche Detectors (PPAD) [10,11] covering $\approx 70\%$ of the forward solid angle. They measured, with very low thresholds (< 0.1 AMeV), impact time and position (FWHM resolution of 600 ps and 3.5 mm, respectively) of heavy reaction products ($A \geq 20$). From the velocity vectors, primary (i.e. pre-evaporative) quantities were deduced, event-by-event, with an improved version [12] of the Kinematic Coincidence Method (KCM).

With respect to previous experiments [13,14], the setup included 160 phoswich scintillators mounted behind most of the PPAD's. They detected LCP's and IMF's with $Z \leq 20$ in $\approx 40\%$ of the forward solid angle (plus a reduced sampling in the backward hemisphere). The phoswiches were two-element modules (fast plastic BC404 + CsI(Tl)) or three-element ones (BC404 + slow plastic BC444 + CsI(Tl)), coupled to fast phototubes. The fast scintillators had been carefully machined down to 200 μm in our workshop, with thickness uniformity better than 5% as required for Z identification up to $Z \approx 20$; the thickness of the BC444 was 5 mm and that of the CsI(Tl) 30 or 50 mm. In the three-element modules, the lack of dead layers and the good optical transmission (obtained by coupling the two plastic elements with the heat-pressing technique) allowed to identify IMF's with low thresholds ($\approx 3-10$ AMeV for $Z=2-20$). The measurement of the time of flight allowed to directly obtain the velocities of LCP's and IMF's, without time consuming and tricky energy calibrations of the scintillators. A detailed description of the apparatus can be found in [15].

The data presented in this Letter are focused on binary

events, where only two major fragments are detected in the PPAD's while the coincident LCP's and IMF's hit the phoswich detectors. Using the Total Kinetic Energy Loss (TKEL) as an ordering variable, it is possible to select events with increasing impact parameter up to grazing collisions. At variance with respect to all available 4π detectors, our low-threshold apparatus makes it possible to measure both the PLF and the TLF also for events with $\text{TKEL} \leq 400$ MeV. Reconstructed primary quantities were obtained from the KCM with 2-body kinematics, not only for LCP, but also for IMF emission [16].

The left panels of Fig. 1 present, for $\text{TKEL}=240\text{-}400$ MeV, the experimental yield of p, d, He and IMF ($Z=3\text{-}7$) in the $V_{\text{perp}} - V_{\text{par}}$ plane, V_{par} and V_{perp} being the center-of-mass velocity components parallel and perpendicular, respectively, to the separation axis of the two major fragments. The dotted lines show the velocity thresholds due to the thickness of the thin plastic scintillator. The data have been corrected for the finite geometry of the apparatus [15]; because of its large acceptance and axial symmetry, the correction is largely independent of the emission pattern. In the backward lab-hemisphere ($V_{\text{par}} \lesssim -40$ mm/ns), owing to the reduced detector coverage, the correction is not as effective as forwards.

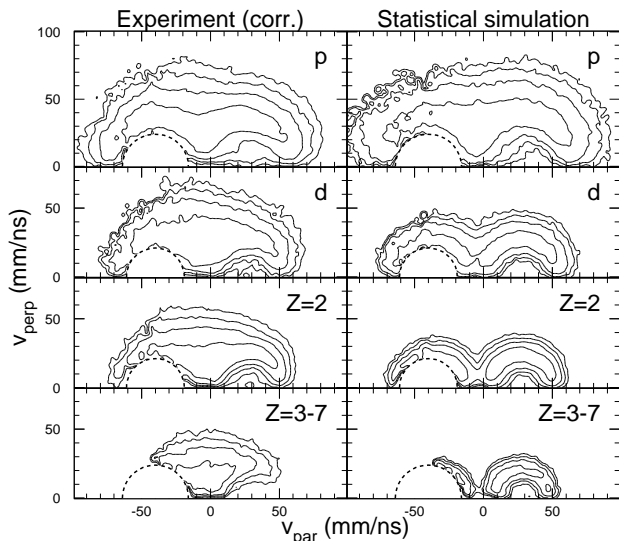


FIG. 1. Left: experimental yields in the $V_{\text{perp}}\text{-}V_{\text{par}}$ plane for p, d, He and IMF's ($Z = 3 - 7$) in the system $^{116}\text{Sn} + ^{93}\text{Nb}$ at 29.5 AMeV, for $\text{TKEL} = 240\text{-}400$ MeV (corrected for the setup geometry). Level spacing is logarithmic, dashed lines indicate velocity thresholds. Right: same results for the simulated statistical emission from the hot reaction partners.

In order to better put into evidence the major features of the experimental data, the right panels of Fig. 1 show the corresponding yields obtained with the simulation of a pure statistical emission from fully accelerated fragments, filtered with the setup acceptance and then corrected as the experimental data. The excitation energy of the fragments was obtained from TKEL with

an “equal energy” sharing, according to [18], while first guesses of the parameters of the evaporation step were deduced from calculations with the code Gemini [17].

The experimental emission pattern for protons does not differ very much from that expected for a sequential evaporation, but with increasing particle mass the mid-velocity yield becomes increasingly important until it actually exhausts most of the IMF intensity.

The mid-velocity particle multiplicities were obtained with a procedure similar to that outlined in [6]. The simulation was tuned so as to reproduce the experimental data in the velocity region corresponding to forward emission from the PLF ($10^\circ \leq \theta_{\text{PLF}} \leq 40^\circ$ in the PLF reference frame). Assuming that the simulation properly mimics the whole statistical emission for PLF and TLF, the mid-velocity yield is obtained as the difference between the total experimental emission and the corresponding estimation of the statistical component.

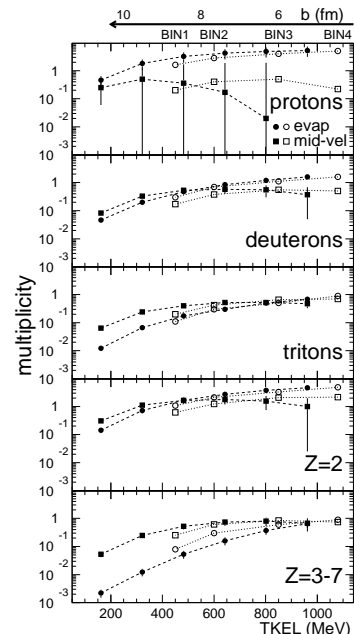


FIG. 2. Experimental multiplicities of p, d, t, He and IMF's ($Z=3\text{-}7$) against TKEL in $^{116}\text{Sn} + ^{93}\text{Nb}$ at 29.5 AMeV. Full squares (circles) refer to the mid-velocity (evaporative) component; open symbols are for the system Xe + Sn at 32 AMeV [7]. Lines are to guide the eye. On top, correspondence between TKEL and impact parameter (or centrality binning of [7]), estimated from the QMD code CHIMERA [19].

The deduced multiplicities are shown as a function of TKEL in Fig. 2, separately for p, d, t, He and IMF. Full circles refer to the statistical evaporation, with uncertainties (due to detector thresholds and determination of the TLF emission) usually smaller than the symbol size. Full squares show the multiplicity of mid-velocity particles. The larger the mid-velocity component, the more reliable its extraction is; the largest errors are for protons, owing to the presence of a large statistical component.

It is worth noting that, in the mid-velocity emission of peripheral events, the mass removed by the IMF's (assuming $A \approx 2Z$) is comparable to that removed by LCP's (while it is much smaller in case of evaporation). Moreover, as already qualitatively seen in Fig. 1, the mid-velocity component of IMF's greatly overcomes the statistical emission, by more than a factor of 20 for the most peripheral collisions. To our knowledge, this extremely enhanced emission of mid-velocity IMF's has never been directly observed before. In these events the nuclear matter tends to break apart in intermediate mass fragments, this process successfully competing with LCP emission.

The comparison of the multiplicities presented in Fig. 2 with those of Xe+Sn (open symbols) at similar bombarding energies [7], requires to find a correspondence between our ordering variable (TKEL) and that (transverse energy of LCP's, $E_{trans12}$) used by the INDRA collaboration to estimate the impact parameter. Following ref. [7], we used the same QMD code CHIMERA [19] as an event generator for our reaction $^{116}\text{Sn} + ^{93}\text{Nb}$. In simulated events, analyzed as the experimental ones, the reconstructed TKEL is narrowly correlated with the impact parameter [20]; details are given in [15]. Here, on top of Fig. 2, we synthetically draw the obtained impact parameter scale, the notation underneath ($BIN1, \dots, BIN4$) corresponding to the binning of [7]. It has to be noted that the range of impact parameters probed by our experiment extends to significantly larger values than those accessible with INDRA, the results of both experiments being in good agreement in the common region.

Addressing the question whether the production mechanism of mid-velocity IMF's is mainly of dynamical or statistical nature is beyond the scope of this letter. However, the peculiar emission pattern observed in the very peripheral collisions (where it is almost free from significant contaminations due to evaporation from PLF and TLF) gives information on the time-space configuration of the emitting system. Namely, it is possible to infer the time scale and the geometrical configuration at the end of the reaction from Coulomb trajectory calculations reproducing the observed emission pattern. Although qualitative descriptions of the IMF emission based on Coulomb trajectory calculations are found in the literature (see, e.g. [21]), quantitative conclusions are not frequent.

A *neck-region emission* was assumed, with the IMF's emitted from a "neck" of excited nuclear matter connecting the two interacting nuclei. Schematically, the Coulomb trajectory calculation was implemented in our Monte Carlo simulation as follows. The two main fragments were assumed to be in an initial configuration (corresponding to the selected peripheral impact parameter) at a distance given by a tuning parameter (d_{sep}) of the calculation. The to-be-emitted IMF, sampled from a realistic distribution, was located in between the two major fragments, with a random "thermal-like" kinetic energy described by another tuning parameter ($\langle E_n \rangle$). The ini-

tial separation velocity of the two main fragments was that appropriate for producing the correct asymptotic TKE. The equations of motion were integrated starting from this simple initial configuration in the three-body phase space, then the experimental filter was applied and the $V_{perp} - V_{par}$ plots were built. Fig. 3a presents the obtained emission pattern for impact parameters corresponding to the experimental data in the bin TKEL=240-400 MeV. The main effect of the two close-lying fragments is to focus the emitted IMF in the transverse direction, with the shape of the V_{perp} distribution mainly depending on the assumed thermal-like energy. In fact, for peripheral collisions, the heavy fragments fly swiftly apart, with no significant energy transfer to the IMF's if they are emitted nearly at rest in the CM system. From the comparison with the experimental correlation (Fig. 3d), one sees that the simulated mechanism of *neck-region emission* significantly contributes to the experimentally observed mid-velocity emission, in particular in the high transverse momentum region, but there is no way to reproduce the two Coulomb-like wings which in the experimental data start at mid-rapidity and rapidly fade away when moving forward (backward) in the PLF (TLF) emission frame.

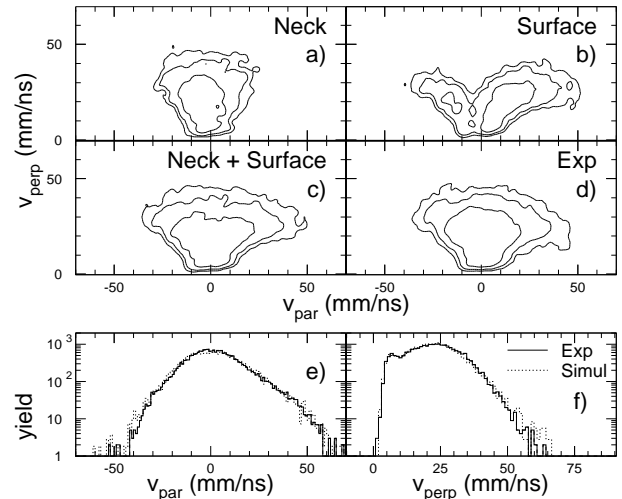


FIG. 3. $V_{perp}-V_{par}$ plots for IMF's ($Z=3-7$) at TKEL=240-400 MeV: (a) Coulomb trajectory calculation with *neck-region emission* with $\langle E_n \rangle = 25$ MeV and (b) for *surface emission* with $\langle E_s \rangle = 10$ MeV, (c) superposition of the two contributions and (d) experimental correlation. Projection of experimental (full histogram) and simulated (dotted histogram) yields on (e) the V_{par} and (f) the V_{perp} axis.

It was therefore assumed that a second contribution exists, similar to the so-called fast oriented fission [11,22] where the very asymmetric fission-like decays of $A \approx 100$ nuclei proceed through nearly aligned configurations (light fission fragment in between the heavier one and the other non-fissioning reaction partner) with characteristic times of the order of $10^{-21} s \approx 300 fm/c$. We performed

Coulomb trajectory calculations assuming a fast *surface emission* of IMF's from the contact regions on the surface of the two flying-apart primary fragments. The IMF was emitted, again with a "thermal-like" energy $\langle E_s \rangle$, from a point of the surface randomly spread within a few fm from the separation axis. The emission pattern obtained for such emissions is presented in Fig. 3b. This *surface* mechanism reproduces the wings of the experimental distribution (Fig. 3d), but not the large transverse energies: in this case the distribution is mainly determined by the Coulomb field of the emitting fragment.

In order to satisfactorily reproduce the experimental data, both contributions must be included. The best agreement with the experiment has been obtained for a ratio between *surface* and *neck-region emission* of 0.7 and with values of $\langle E_s \rangle = 10$ MeV and $\langle E_n \rangle = 10$ MeV: the result is shown in Fig. 3c. The projections of the experimental data and the simulation (continuous and dotted histograms, respectively) on the V_{par} (Fig. 3e) and V_{perp} (Fig. 3f) axes allow to better perceive the good quality of the obtained agreement. In both projections, the simulation presents a sizeable sensitivity to the assumed random energies $\langle E_n \rangle$ and $\langle E_s \rangle$. In fact, a change of 5 MeV in these parameters worsens in a significant way the agreement. An agreement of the same quality is found for more peripheral events ($TKEL \leq 240$ MeV), while for more central TKEL-bins the comparison becomes increasingly blurred by the growing contribution of the statistical emission. The overall trend is that both the random energy $\langle E_n \rangle$ of the *neck-region emission* and the spread of the emission point in the *surface emission* increase with increasing centrality.

For peripheral events, the experimental IMF emission appears to be compatible with the formation of a neck-like structure which then decays by a prompt emission from the neck region itself or by a successive emission from the surfaces of the separating nuclei. For example, the *neck-region emission* may be due to a multiple neck rupture, while the *surface emission* is suggestive of a single neck rupture [23], leaving one of the main fragments in a rather deformed shape, in the vicinity (or even beyond) its saddle shape. In the simulation these two mechanisms differ in terms of the initial configuration: the *neck-region emission* contributes at small distances d_{sep} compatible with the presence of a connecting neck, the *surface emission* at larger distances. According to models quantitatively describing the formation of the neck in nuclear collisions or fission [23], the maximum length of the neck –discriminating between the two mechanisms– was estimated to be 12 fm . From the relative kinetic energy at separation and from the envisaged geometrical configuration, it is possible to estimate the time scale: a value of the order of 60 fm/c is obtained as a discrimination between *neck-region* and *surface emission*. Moreover, from the observed anisotropy and using realistic values of the angular momenta and moments of inertia of the nuclei,

one can exclude for the *surface emission* times significantly larger than a few hundreds of fm/c .

In conclusion, peripheral collisions are characterized by an important emission of IMF's at mid-velocity, successfully competing with LCP's. Indications for a fast energy dissipation process of locally excited nuclear matter may be inferred from the estimated *thermal-like* energies necessary to reproduce the data. The emission pattern of IMF's is compatible with the coexistence of two mechanisms of prompt or fast emission: the first one related to the formation and prompt break-up of a neck of highly excited nuclear matter and the second one, at a somewhat later stage, characterized by a localized emission from the possibly highly deformed flying apart fragments.

We wish to thank J. Lukasik for providing us with the QMD code CHIMERA. We are grateful to R. Ciaranfi and M. Montecchi for the development of dedicated electronics, and to P. Del Carmine for his help in the setup preparation. Many thanks are due to L. Calabretta and to the whole machine crew of the LNS for their continuous efforts to provide a good quality pulsed beam.

-
- [1] D.R. Bowman *et al.*, Phys. Rev. Lett. **70**, 3534 (1993).
 - [2] C.P. Montoya *et al.*, Phys. Rev. Lett. **73**, 3070 (1994).
 - [3] J. Töke *et al.*, Phys. Rev. Lett. **75**, 2920 (1995).
 - [4] J.F. Dempsey *et al.*, Phys. Rev. C **54**, 1710 (1996).
 - [5] J. Töke *et al.*, Phys. Rev. Lett. **77**, 3514 (1996).
 - [6] J. Lukasik *et al.*, Phys. Rev. C **55**, 1906 (1997).
 - [7] E. Plagnol *et al.*, Phys. Rev. C **61**, 014606 (1999).
 - [8] G. Poggi, Nucl. Phys. A **685**, 296c (2001).
 - [9] A. Botvina *et al.*, Phys. Rev. C **59**, 3444 (1999).
 - [10] R.J. Charity *et al.*, Z. Phys. A **341**, 53 (1991).
 - [11] A.A. Stefanini *et al.*, Z. Phys. A **351**, 167 (1995).
 - [12] G. Casini *et al.*, Nucl. Instr. Meth. A **277**, 445 (1989).
 - [13] G. Casini *et al.*, Phys. Rev. Lett. **78**, 828 (1997).
 - [14] G. Casini *et al.*, Phys. Rev. Lett. **83**, 2537 (1999).
 - [15] S. Piantelli, Ph.D. Thesis, Firenze 2001, and to be published.
 - [16] It was checked that in case of emission of just one IMF (the average IMF multiplicity is well below 1 for semiperipheral collisions) good agreement is found between the results of the analysis with the 2-body kinematics (ignoring the IMF) and with the 3-body kinematics (including the IMF as a third body).
 - [17] R.J. Charity *et al.*, Nucl. Phys. A **483**, 371 (1988).
 - [18] G. Casini *et al.*, Europ. Phys. Jour. A **9**, 491 (2000).
 - [19] J. Lukasik and Z. Majka, Acta Phys. Pol. B **24**, 1959 (1993).
 - [20] The same analysis showed that, because of the reduced acceptance of our setup, the $E_{trans12}$ selection gave no narrow correlation with the impact parameter.
 - [21] J. Töke *et al.*, Nucl. Phys. A **583**, 519 (1995).
 - [22] G. Casini *et al.*, Phys. Rev. Lett. **71**, 2567 (1993).
 - [23] U. Brosa and S. Grossmann, J. Phys. G **10**, 933 (1984).